Anaphase promoting complex–dependent degradation of transcriptional repressors Nrm1 and Yhp1 in *Saccharomyces cerevisiae*

Denis Ostapenko and Mark J. Solomon
Department of Molecular Biophysics and Biochemistry, Yale University, New Haven, CT 06520-8114

ABSTRACT **The anaphase-promoting complex/cyclosome (APC/C) is an essential ubiquitin ligase that targets cell cycle proteins for proteasome-mediated degradation in mitosis and G1. The APC regulates a number of cell cycle processes, including spindle assembly, mitotic exit, and cytokinesis, but the full range of its functions is still unknown. To better understand cellular pathways controlled by the APC, we performed a proteomic screen to identify additional APC substrates. We analyzed cell cycle–regulated proteins whose expression peaked during the period when other APC substrates were expressed. Subsequent analysis identified several proteins, including the transcriptional repressors Nrm1 and Yhp1, as authentic APC substrates. We found that APC^{Cdh1} targeted Nrm1 and Yhp1 for degradation in early G1 through Destruction-box motifs and that the degradation of these repressors coincided with transcriptional activation of MBF and Mcm1 target genes, respectively. In addition, Nrm1 was stabilized by phosphorylation, most likely by the budding yeast cyclin–dependent protein kinase, Cdc28. We found that expression of stabilized forms of Nrm1 and Yhp1 resulted in reduced cell fitness, due at least in part to incomplete activation of G1-specific genes. Therefore, in addition to its known functions, APC-mediated targeting of Nrm1 and Yhp1 coordinates transcription of multiple genes in G1 with other cell cycle events.**

Monitoring Editor
Daniel Lew
Duke University

Received: Jan 11, 2011
Revised: May 3, 2011
Accepted: May 5, 2011

INTRODUCTION

Cell cycle progression requires the coordinated degradation of key regulatory proteins by the ubiquitin-proteasome pathway. Protein ubiquitination occurs in a series of reactions carried out by three proteins: an E1 (ubiquitin-activating enzyme), an E2 (ubiquitin-conjugating enzyme), and an E3 (ubiquitin ligase). The resulting covalent formation of polyubiquitin chains targets proteins for degradation by the 26S proteasome (Kerscher *et al.*, 2006). Two major classes of RING-type E3s play critical roles during the cell division cycle. These are the anaphase-promoting complex/cyclosome (APC/C) and the Skp1-Cullin-F-box protein complex (SCF), each of which binds protein substrates and mediates their interaction with the ubiquitin-loaded E2 (Petroski and Deshaies, 2005; Peters, 2006; Thornton *et al.*, 2006).

In vegetative cells, the APC is a large complex composed of 13 distinct core proteins plus a WD40 repeat–containing activator, either Cdc20 or Cdh1. Both Cdc20 and Cdh1 bind APC substrates through their degradation motifs, principally a Destruction box (D-box; RxxLxxxxN) and a KEN-box (Glotzer *et al.*, 1991; Pfleger and Kirschner, 2000; Burton and Solomon, 2001). Mutations within these motifs prevent substrate recognition that leads to increased protein stability. In addition, a nonsubstrate binding function for Cdc20 has been suggested (Kimata *et al.*, 2008a). The activity of the APC is itself tightly regulated. Cdc20 is degraded during G1 in an APC^{Cdh1}-dependent manner and is inhibited during mitosis by the spindle assembly checkpoint, which ensures that all chromosomes are properly attached to the mitotic spindle before the onset of anaphase (Fang *et al.*, 1998; Hwang *et al.*, 1998; Yu, 2002; Burton and Solomon, 2007). Cdh1 is inhibited by phosphorylation by cyclin-dependent protein kinases and polo-like kinases and by

This article was published online ahead of print in MBoC in Press (http://www.molbiolcell.org/cgi/doi/10.1091/mbc.E11-01-0031) on May 11, 2011.

The authors declare they have no conflict of interest.

Address correspondence to: Mark J. Solomon (Mark.Solomon@yale.edu).

Abbreviations used: APC/C, anaphase-promoting complex/cyclosome; Cdk, cyclin-dependent protein kinase; CM, complete minimal; D-box, Destruction box motif; DMSO, dimethyl sulfoxide; DTT, dithiothreitol; mdb, mutant destruction box; mkb, mutant KEN-box; PAP, peroxidase–antiperoxidase; PMSF, phenylmethylsulfonyl fluoride; qRT PCR, quantitative reverse transcriptase PCR; SCF, Skp1-Cullin-F-box; TAP, tandem-affinity purification; YPD, yeast extract–peptone–dextrose.

the binding of pseudosubstrate inhibitors that interact with Cdh1 through degradation-like motifs and thereby prevent Cdh1 from binding to its substrates (Zachariae *et al.*, 1998; Jaspersen *et al.*, 1999; Reimann *et al.*, 2001; Di Fiore and Pines, 2007; Enquist-Newman *et al.*, 2008; Kimata *et al.*, 2008b; Ostapenko *et al.*, 2008). Thus Cdc20 activity is limited to mitosis and Cdh1 activity is limited to the end of mitosis and G1.

Several budding yeast APC substrates coordinate transitions between stages of the cell cycle. For example, the assembly and stability of the mitotic spindle is regulated by Cdh1-mediated degradation of two kinesins—Cin8 and Kip1—and two microtubule-associated proteins—Ase1 and Fin1 (Juang *et al.*, 1997; Shirayama *et al.*, 1998; Hildebrandt and Hoyt, 2001; Woodbury and Morgan, 2007). Cdc20 is an essential protein; of the known APC^{Cdc20} substrates, degradation of Pds1/Securin and Clb5 is essential for cell viability (Shirayama *et al.*, 1998; Thornton and Toczyski, 2003). In contrast, cells lacking Cdh1 are viable, although deletion of Cdh1 leads to various morphological defects. Since stabilization of individual APC^{Cdh1} substrates has only modest effect, it appears that the combined and coordinated degradation of multiple APC^{Cdh1} substrates is essential for normal cell growth.

Both ubiquitin-mediated proteolysis and transcriptional regulation contribute to the periodic expression of cell cycle proteins. Two examples of transcriptional regulation are relevant to our studies. When environmental and internal conditions are favorable for cell growth, the MADS box protein Mcm1 initiates transcription of G1-specific genes such as *CLN3*, which encodes a cyclin, and other genes required for prereplication complex assembly (Pramila *et al.*, 2002). Transcriptional activation of these genes by Mcm1 is limited to G1, even though Mcm1 remains associated with target gene promoters throughout the cell cycle. Outside G1, Mcm1 is inhibited by two homeodomain proteins, Yox1 and Yhp1, that bind to adjacent sites within gene promoters (Pramila *et al.*, 2002). The MBF complex (composed of Mbp1 and Swi6) also initiates in G1 the transcription of genes required for DNA replication and progression into S phase. Outside G1, MBF is negatively regulated by Nrm1, which binds to MBF-regulated promoters and interacts directly with Mbp1 (de Bruin *et al.*, 2006). *NRM1* transcription is up-regulated by MBF, providing a negative feedback loop to control MBF activity.

To better understand cell cycle processes regulated by ubiquitin-mediated protein degradation, we sought to identify additional substrates of the APC. By screening short-lived proteins expressed at the same time as known APC substrates, we identified six novel APC substrates. We focused on two of these substrates, the transcriptional repressors Nrm1 and Yhp1. APC^{Cdh1}-mediated degradation of Nrm1 and Yhp1 coincided with transcriptional activation of MBF and Mcm1 targets. In contrast, stabilization of Nrm1 and Yhp1 suppressed the expression of G1-specific targets of MBF and Mcm1, respectively, and reduced the fitness of the mutant strains. Thus, in addition to its known roles, APC^{Cdh1} also contributes to the coordination of gene transcription in G1 with other cell cycle events.

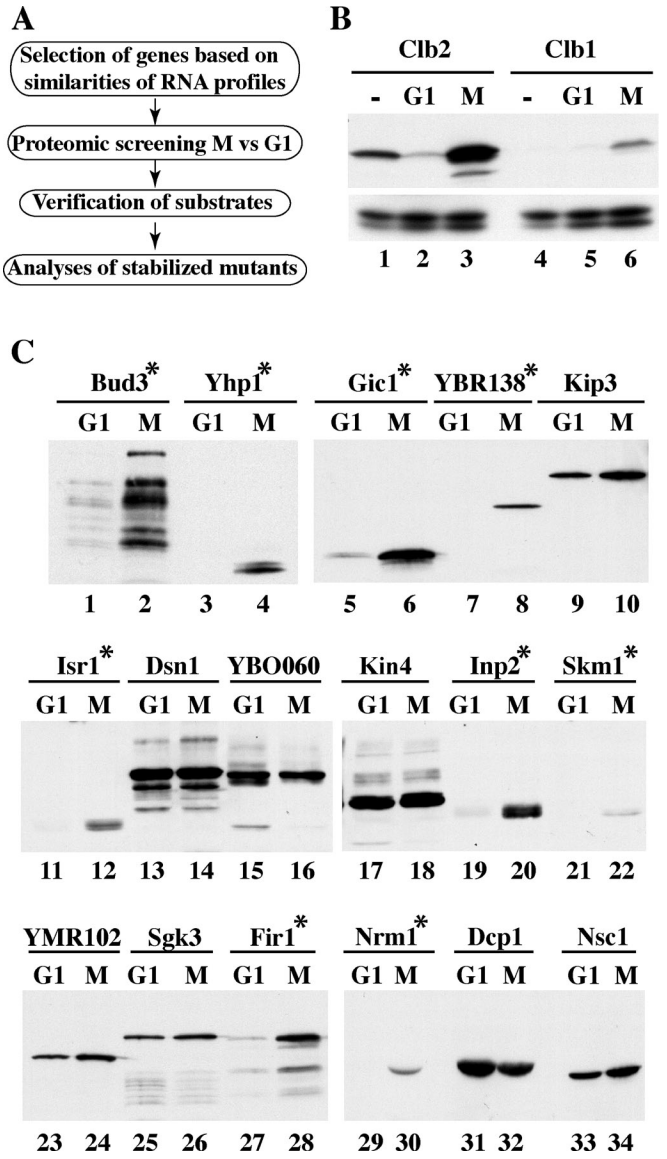

FIGURE 1: Expression-based screening for potential APC substrates. (A) Flowchart showing the analysis of potential APC substrates. (B) The expression levels of endogenous Clb2-TAP and Clb1-TAP in extracts from asynchronous cells (lanes 1 and 4), cells arrested in G1 (lanes 2 and 5), and cells arrested in mitosis (lane 3 and 6) were compared by immunoblotting with anti-TAP antibodies. As a loading control, the membranes were reprobed with anti-PSTAIR antibodies to detect Cdc28 (lower panel). (C) Strains carrying selected TAP-tagged proteins were arrested in G1 and mitosis as above. Proteins that were at least threefold more abundant in benomyl-arrested cells than in G1-arrested cells (*) were considered potential candidates for further analyses.

RESULTS

Screening for candidate APC substrates: G1-unstable proteins

We set out to identify novel APC substrates and to determine the function served by their degradation. We noticed that the transcription of all known APC substrates in budding yeast is cell cycle regulated and falls into two clusters, one with a peak in G2 (*CLB2*, *CDC5*, and *ASE1*), the other with a peak in G1 (*CIN8*, *FIN1*, and *KIP1*; Spellman *et al.*, 1998; Pramila *et al.*, 2006). This coherent regulation suggested that additional APC substrates might have similar mRNA profiles. In addition, a genome-wide study found that most of the known substrates were relatively unstable proteins even in asynchronous cells (Belle *et al.*, 2006). Thus we identified genes that were cotranscribed with known APC substrates (Spellman *et al.*, 1998). At a later stage of this study, we added additional candidates from a finer transcriptional analysis (Pramila *et al.*, 2006), paying particular attention to proteins reported to have short half-lives (Belle *et al.*, 2006). Of this smaller collection, we analyzed those that were present in a tandem-affinity purification (TAP)-tag library representing ~80% of all genes in *Saccharomyces cerevisiae* (Ghaemmaghami *et al.*, 2003). In total, we analyzed 134 proteins following the flowchart in Figure 1A.

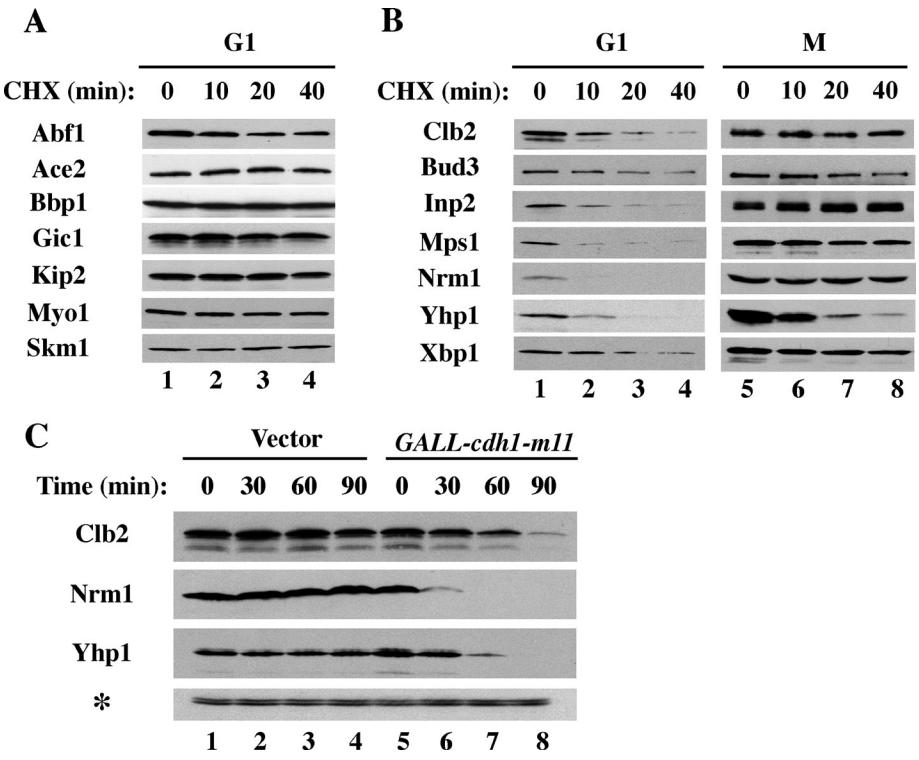

FIGURE 2: Screening for proteins that are unstable in G1 but stable in mitosis. (A) Cells expressing the endogenously TAP-tagged proteins (as labeled) were arrested in G1 and treated with 500 μg/ml cycloheximide. Samples were withdrawn at the indicated times and processed for immunoblotting to detect TAP-tagged proteins. These proteins were stable and not considered further as potential APC substrates. (B) As in (A) but the stabilities of these proteins were analyzed both in G1 (as above) and in cells arrested in mitosis (M) by incubation with 20 μg/ml benomyl. Most of the proteins shown were unstable in G1 but stabilized in M phase, as expected for APC substrates. (C) *cdh1-m11* targets Nrm1 and Yhp1 for unscheduled degradation. Cells carrying an empty vector or *GALLp-cdh1-m11* were grown in the presence of raffinose and induced with 2% galactose for the indicated times. Cdh1-m11 lacks sites of inhibitory phosphorylation and is constitutively active. Samples were processed for immunoblotting to examine the endogenous levels of Clb2, Nrm1, and Yhp1. Cdc28 (*) was used as a loading control.

To quickly eliminate those proteins that were clearly not APC substrates, we screened this collection for proteins that were more abundant during M phase (in cells arrested by the spindle assembly checkpoint following microtubule depolymerization by benomyl) than in G1 (in cells arrested with the mating pheromone α-factor). All known APC^{Cdc20} and APC^{Cdh1} substrates fit this pattern. To verify the validity of this approach, we first examined the levels of a few known APC substrates that were expressed from their native promoters as TAP-tagged fusions, which facilitated detection by immunoblotting. As expected, we found that the levels of Clb2, Clb1, Cdc5, Cin8, and Spo12 were severalfold higher in benomyl-arrested cells than in G1 cells (Figure 1B; unpublished data). We then treated strains containing TAP-tagged versions of each of the selected 134 proteins with benomyl or with α-factor and assessed the levels of each protein by immunoblotting (Figure 1C). Several low-abundance proteins were concentrated by immunoprecipitation prior to immunoblotting to increase the sensitivity of their detection. For each protein, we calculated an M/G1 ratio to assess which proteins were depleted from G1-arrested cells. Out of 134 proteins examined, 31 were more than threefold more abundant in M phase than in G1 phase, four were more abundant in G1, 89 were present at similar levels in M and G1, and 10 were undetectable (Supplemental Table I).

Excluding five previously identified APC substrates, we determined which of the 26 proteins that were more abundant in M phase than in G1 were unstable by using a series of cycloheximide time-course experiments. We found that 15 of these proteins were completely stable in G1 phase (Figure 2A; unpublished data), suggesting that their apparent differences in protein abundance were due to variable gene transcription or induction in the presence of benomyl. In contrast, 11 proteins were highly unstable in G1 phase, with apparent half-lives ranging from 5 to 15 min (Figure 2B; unpublished data). Some of these proteins were difficult to detect even at time zero, presumably due to protein degradation before the beginning of the time course. We also determined the stabilities of these 11 proteins in benomyl-arrested cells in M phase (Figure 2B), during which APC substrates should be stable. Indeed, Clb2 and six other proteins were significantly stabilized. In contrast, Yhp1 and several other proteins remained unstable in M phase, indicating that their turnover during M phase involves a ubiquitin ligase other than the APC. As we will discuss below (Figure 3D), we believe that Yhp1 is both an APC substrate in G1 and a substrate for an additional ubiquitin ligase.

Additional evidence that APC was directly involved in targeting of the identified proteins was obtained using a constitutively active form of Cdh1, cdh1-m11, which carries substitutions within 11 phosphoacceptor sites, rendering it refractory to Cdc28-mediated inhibition (Zachariae *et al.*, 1998). Expression of cdh1-m11 caused a rapid decline in the levels of Nrm1 and Yhp1 (Figure 2B) comparable to the rapid decline cdh1-m11 induction caused for Clb2 (Figure 2B). On the basis of the differential stabilities in G1 and M phase and sensitivity to cdh1-m11 expression, we considered six proteins to be potential APC substrates. We previously reported a characterization of one of these proteins, Iqg1, as an APC substrate (Ko *et al.*, 2007). We decided to investigate two of these proteins—Nrm1 and Yhp1—in more detail, as they have both been implicated in control of transcriptional repression, which has not previously been attributed to APC-mediated regulation. The characterization of other substrates from this screen will be reported elsewhere.

APC^{Cdh1}-dependent degradation of Nrm1 and Yhp1

To determine directly if the APC promoted the degradation of Nrm1 and Yhp1, we carried out half-life experiments in G1-arrested wild-type and APC mutant (*cdh1Δ*) cells. Following transient expression to approximately physiological levels, we found that Nrm1 and Yhp1 were rapidly degraded in wild-type cells but significantly stabilized in *cdh1Δ* cells (Figure 3, A and D). Nrm1 was also stabilized in a conditional APC mutant strain (*cdc23–1*), but we were unable to test the degradation of Yhp1 in *cdc23–1* cells due to the incomplete G1 arrest of this strain prior to galactose addition (unpublished data).

We sought to identify the degradation motif(s) in Nrm1. It has been reported that deletion of the 13 N-terminal amino acids of

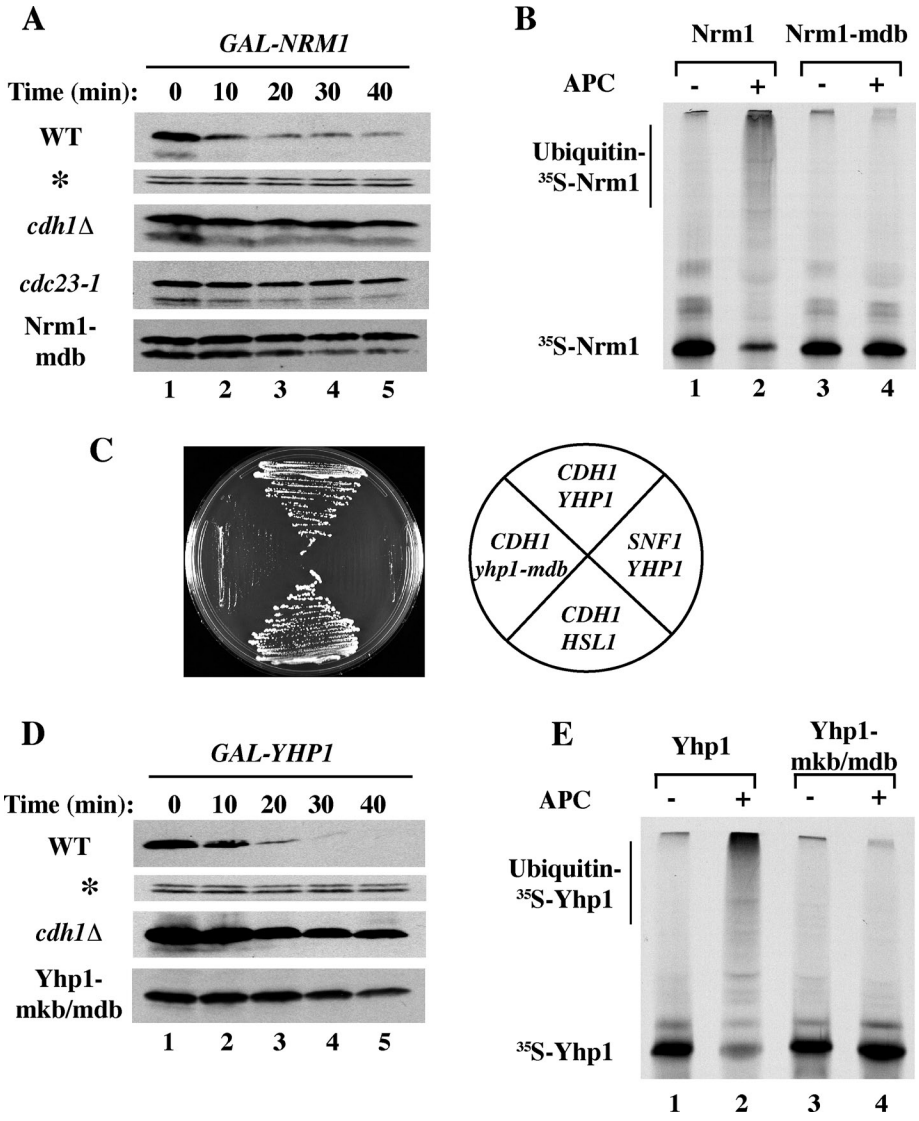

FIGURE 3: APC-dependent ubiquitination of Nrm1 and Yhp1. (A) Wild-type and *cdc23–1* cells were arrested in G1 with α-factor and transferred to the nonpermissive temperature to inactivate Cdc23, a core subunit of the APC. *cdc28–13 cdh1*Δ cells were arrested in G1 by incubation at the nonpermissive temperature for *cdc28–13*. A putative D-box within Nrm1, ^{7}RLPL, was mutated to generate Nrm1-mdb. The expression of *NRM1* and *nrm1-mdb* were induced from *GAL1p* for 45 min followed by addition of 2% dextrose and 500 μg/ml cycloheximide to terminate protein synthesis. Samples were withdrawn at the indicated times and processed for immunoblotting with anti-TAP antibodies. Cdc28 (*) was used as a loading control. (B) Ubiquitination of Nrm1 in vitro. Nrm1 and Nrm1-mdb were synthesized in vitro in the presence of [^{35}S]methionine and tested for ubiquitination in the absence (lanes 1 and 3) or presence (lanes 2 and 4) of purified APC and Cdh1. (C) Yeast two-hybrid interactions between Cdh1 and Yhp1. Cells expressing *CDH1-ΔN200-DB* or *SNF1-DB* (as a negative control) and *YHP1-AD*, *HSL1-AD*, or *yhp1-mkb/mdb-AD* were tested for growth on selective medium, which indicates interaction of the respective proteins. (D) Two potential degradation motifs, ^{329}KEN-box and ^{340}RKPL within Yhp1, were altered to generate Yhp1-mkb/mdb. Half-lives of Yhp1 and Yhp1-mkb/mdb in G1 were determined as in (A). Samples were withdrawn at the indicated times and processed for immunoblotting to detect Yhp1-TAP. (E) Ubiquitination of Yhp1 in vitro. ^{35}S-labeled Yhp1 and Yhp1-mkb/mdb were tested for ubiquitination in the absence (lanes 1 and 3) or presence (lanes 2 and 4) of APC and Cdh1 as in (B).

Nrm1 leads to its stabilization (de Bruin *et al.*, 2006). In agreement, we found that mutation of a potential N-terminal D-box, ^{7}RLPL, was sufficient to stabilize Nrm1 (Figure 3A, lower panel). Mutation of a second potential D-box, ^{151}RRKL, or deletion of *cdh1*Δ did not further stabilize Nrm1-mdb (unpublished data). ^{35}S-labeled Nrm1 was efficiently ubiquitinated by APC^{Cdh1} in vitro, as revealed by the appearance of high-molecular-weight ubiquitin-Nrm1 conjugates and loss of unmodified Nrm1 (Figure 3B, lanes 1–2). In contrast, Nrm1-mdb was not ubiquitinated (Figure 3B, lanes 3–4). Consistent with this role for the N-terminal D-box, expression of *nrm1-mdb* from its own promoter led to a significant elevation in Nrm1 relative to the wild-type protein (unpublished data).

We identified potential degradation motifs in Yhp1 using a yeast two-hybrid assay for interaction with Cdh1. In this assay, Cdh1-ΔN200 (which lacks the first 200 amino acids of Cdh1) interacted strongly and specifically with Hsl1, a known APC substrate (J. Burton and M. J. Solomon, unpublished observations). We found that the interaction of Yhp1 with Cdh1 in this assay was mediated by Yhp1's C-terminal KEN-box and D-box (Figure 3C). To test whether these motifs contribute to the degradation of Yhp1 via APC^{Cdh1}, we mutated ^{329}KEN (mkb) and ^{340}RKPL and assessed the stability of the resulting protein in a promoter shutoff assay in G1 cells. We found that Yhp1-mkb/mdb was highly stabilized compared with wild-type Yhp1 (Figure 3D, lower panel). The continued slow degradation of Yhp1-mkb/mdb was likely due to the APC^{Cdh1}-independent pathway that degrades Yhp1 in checkpoint-arrested cells (see Figure 2B). A second potential D-box, ^{203}RIEL, does not seem to contribute to Yhp1 degradation (unpublished data). We next tested whether ^{35}S-labeled Yhp1 could be ubiquitinated by APC^{Cdh1} in vitro using purified components. Wild-type Yhp1 was very efficiently ubiquitinated, as revealed by the appearance of high-molecular-weight ubiquitin-Yhp1 conjugates and the strong depletion of unmodified Yhp1 (Figure 3E, lanes 1 and 2). In contrast, Yhp1-mkb/mdb was not ubiquitinated (Figure 3E, lanes 3 and 4). Thus Nrm1 and Yhp1 are degraded in an APC^{Cdh1}-dependent manner in G1 in a reaction that requires an intact D-box in Nrm1 and a C-terminal D-box and KEN-box in Yhp1.

Cdh1 targets Nrm1 and Yhp1 in cycling cells

We next explored the role of the APC in the degradation of Nrm1 and Yhp1 upon exit from M phase. We first arrested cells in anaphase following inactivation of *cdc15–2*, released cells from the arrest, and followed Nrm1 levels through the next cell cycle (Figure 4A). Although Nrm1 levels declined 20 and 40 min after release of *cdc15–2* cells (Figure 4A, lanes 1–3), there was little change in Nrm1 level after release of *cdc15–2 cdh1*Δ double-mutant cells (Figure 4A, lanes 6–8), indicating that APC^{Cdh1} was largely responsible for the observed Nrm1

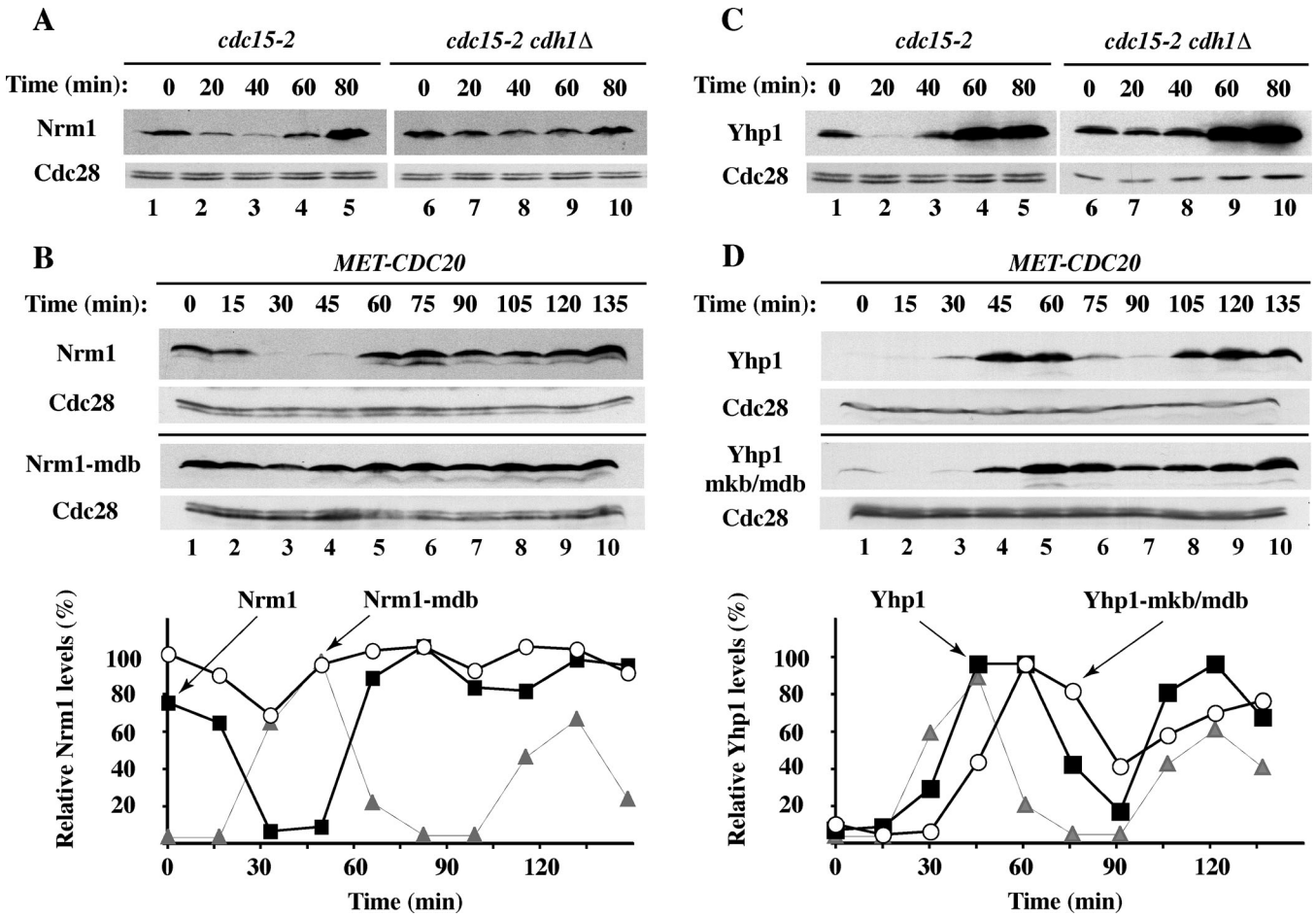

FIGURE 4: Nrm1 and Yhp1 are degraded in G1 in a Cdh1-dependent manner. (A) *cdc15–2* and *cdc15–2 cdh1*Δ cells carrying endogenous *NRM1-TAP* were synchronized in mitosis by incubation at 37°C for 3 h. Samples were withdrawn at the indicated times following release at 23°C and processed for immunoblotting to detect Nrm1-TAP. (B) *MET-CDC20* cells carrying endogenous *NRM1* or *nrm1-mdb* were synchronized in mitosis by incubation with 5 mM methionine for 2.5 h to deplete Cdc20. Cells were released from the arrest into methionine-free medium at time zero and samples were taken at the indicated times and processed for immunoblotting to detect Nrm1-TAP. Normalized levels of Nrm1 (solid squares) and Nrm1-mdb (open circles) were plotted below. The percentages of cells with anaphase spindles (shaded triangles) are indicated. (C) Yhp1 is degraded via APC^{Cdh1} upon anaphase exit. *cdc15–2* and *cdc15–2 cdh1*Δ cells carrying endogenous *YHP1-TAP* were synchronized and released from mitosis as in (A). Samples were withdrawn at the indicated times and processed for immunoblotting to detect Yhp1-TAP. (D) *MET-CDC20* strains expressing endogenous *YHP1* or *yhp1-mkb/mdb* were synchronized in mitosis as in (B). Samples were processed to detect Yhp1; Cdc28 was used as a loading control. Normalized levels of Yhp1 (solid squares) and Yhp1-mkb/mdb (open circles) are plotted. The percentages of cells with anaphase spindles (shaded triangles) are indicated.

degradation. We also examined Nrm1 levels following synchronization of cells in mitosis by depletion of Cdc20. Wild-type Nrm1 was undetectable 30 min after release from this arrest, reappeared at 60–75 min, and subsequently declined during the next G1 (Figure 4B, upper panel). In contrast, Nrm1-mdb levels decreased only slightly in G1 and remained elevated compared with that of wild-type Nrm1 (Figure 4B, lanes 4 and 8, and graph). Thus mutation of the Nrm1 D-box significantly extends Nrm1 presence in G1, a phase when it is normally absent.

We performed a similar analysis of Yhp1 following cell synchronization in mitosis. We first examined Yhp1 levels in cells arrested in anaphase by *cdc15–2* inactivation and released into a synchronous cell cycle. Although Yhp1 levels were low during the anaphase arrest, at least some protein persisted through mitosis and was degraded after release of *cdc15–2* cells from the arrest (Figure 4C, lanes 1 and 2). In contrast, there was little degradation of Yhp1 following release of *cdc15–2 cdh1*Δ cells (Figure 4C, compare lanes 2 and 7), indicating that the observed degradation of Yhp1 in early G1 was Cdh1-dependent. We also examined Yhp1 levels in cells synchronized by Cdc20 depletion. Yhp1 levels were low in mitosis, accumulated 45–60 min after the release, and then decreased in the following mitosis and G1 (Figure 4D). Although Yhp1-mkb/mdb levels also cycled, there were clear differences in the profiles of Yhp1 and Yhp1-mkb/mdb, including an increased abundance of Yhp1-mkb/mdb at 75–90 min and an elevated nadir between peaks (Figure 4D, lanes 6–7, and graph). Thus APC^{Cdh1} appears to eliminate any Yhp1 remaining from the previous mitosis.

Nrm1 stability is controlled by Cdh1 and Cdc28

Because Nrm1 contains several Ser-Pro/Thr-Pro consensus cyclin-dependent protein kinase (Cdk) phosphorylation sites, and because a previous study demonstrated that the Cdc28 protein kinase could phosphorylate Nrm1 in vitro (Ubersax *et al.*, 2003), we investigated whether Cdc28 might regulate Nrm1 stability. We

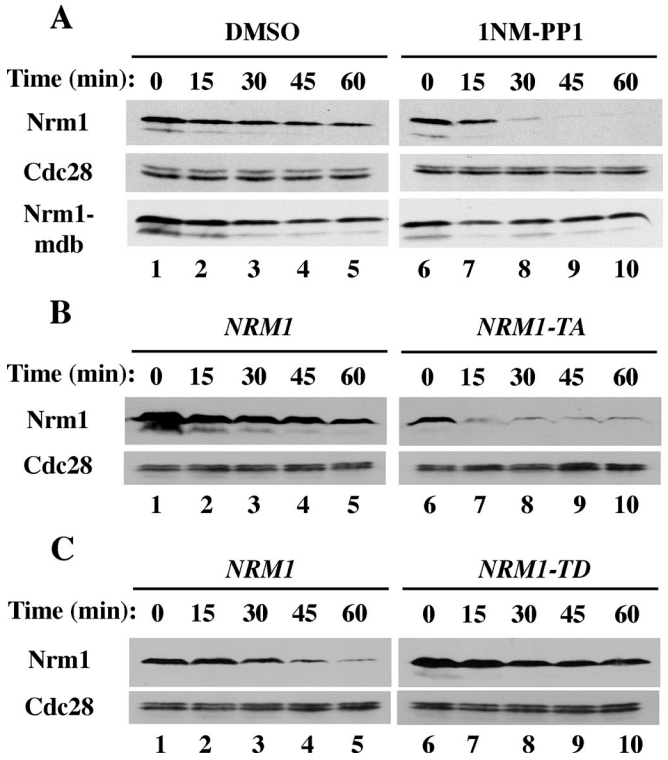

FIGURE 5: Cdc28-mediated phosphorylation regulates Nrm1 stability. (A) *GAL1p-NRM1* and *nrm1-mdb* were expressed in asynchronous *cdc28-as* cells in the presence of 2% galactose for 45 min followed by the addition of dimethyl sulfoxide (DMSO) (lanes 1–5) or 1 μM 1NM-PP1 (to inhibit Cdc28-as; lanes 6–10) for the last 10 min of galactose induction. The degradation of Nrm1 and Nrm1-mdb were examined following the addition of 2% dextrose and 500 μg/ml cycloheximide as in Figure 3A. (B) Four potential Cdc28 phosphorylation sites within Nrm1 were mutated to generate Nrm1–4TA. *GALp-NRM1* and *NRM1-4TA* were expressed in asynchronous cells and Nrm1 and Nrm1-4TA degradation were examined as in (A). (C) The four potential Cdc28 phosphorylation sites were mutated to aspartic acid to generate Nrm1-4TD and the stabilities of Nrm1 and Nrm1-4TD in G1-arrested cells was assessed as in (B).

examined Nrm1 stability in *cdc28-as* cells containing a mutant form of Cdc28 that can be inhibited rapidly by the bulky ATP analogue, 1NM-PP1 (Bishop *et al.*, 2000). Nrm1 levels declined rapidly after addition of 1NM-PP1 to an asynchronous population of *cdc28-as* cells (Figure 5A, lanes 6–10). In contrast, Nrm1-mdb was not significantly destabilized under the same conditions, indicating that decreased Cdc28 activity promoted Nrm1 degradation in a D-box-dependent manner. To examine whether the effect of Cdc28 inhibition on Nrm1 might be direct, we mutated four potential Cdk sites within Nrm1. Mutations of the evolutionarily conserved ^{163}TPAR, ^{171}TPSS, ^{207}TPIR, and ^{231}TPTS sites (to produce Nrm1–4TA) significantly reduced Nrm1 stability (Figure 5B). Although Nrm1-TA was expressed at low levels, introduction of a D-box mutation (Nrm1-TA-mdb) resulted in normal expression (unpublished data). Furthermore, mutations of the four Cdk consensus phosphorylation sites to aspartic acid residues to mimic phosphorylated threonine resulted in increased stability compared with wild-type Nrm1 in G1-arrested cells (Figure 5C). Thus it appears that phosphorylation of Nrm1, likely by Cdc28, protects Nrm1 from Cdh1-mediated degradation.

Stabilized versions of Nrm1 and Yhp1 repress G1 transcription and decrease cell fitness

Since Nrm1 and Yhp1 are transcriptional repressors, we tested whether their stabilization might alter the expression of target G1 genes. We first monitored transcription of *RNR1*, one of the best-characterized MBF targets, in populations of wild-type and *nrm1-mdb* cells synchronized in mitosis by Cdc20 depletion. Real-time PCR analysis revealed that in wild-type cells, *RNR1* transcription initiated in G1, ~30 min after release from mitotic arrest, and declined at 60 min, as cells entered S phase (Figure 6A, Top). Thus, as expected (de Bruin *et al.*, 2006), there was an inverse correlation between the presence of Nrm1 and transcription of *RNR1*. In contrast, although *RNR1* transcription began promptly in G1 in *nrm1-mdb* cells, it terminated prematurely, reducing both the duration and maximal level of *RNR1* expression compared with wild-type cells (Figure 6A, Top). This effect was observed in three independent experiments and was confirmed by Northern blotting analysis (Figure 6C, Top and Middle). These findings are in agreement with previous results showing that overexpression of an N-terminally truncated form of Nrm1 attenuated *RNR1* expression and increased the hydroxyurea sensitivity of the cells (de Bruin *et al.*, 2006). We also found that transcription of *CDC21*, another MBF target, was terminated prematurely in *nrm1-mdb* cells, whereas transcription of *CLB2*, which is regulated independently of MBF, was not affected (Figure 6A, Middle and Bottom).

We performed a similar analysis in cells expressing the stabilized form of Yhp1. We hypothesized that expression of endogenous Yhp1-mkb/mdb might affect expression of *RNR1* and *MCM7*, since constitutive overexpression of *YHP1* leads to repression of these genes (Chua *et al.*, 2006). Indeed, the duration and expression levels of *RNR1* and *MCM7* transcription in *yhp1-mkb/mdb* mutant cells were reduced compared with wild-type cells (Figure 6B, Top and Middle, and Figure 6C, Bottom). As expected, transcription of *CLB2*, which is independent of Yhp1, was not affected (Figure 6B, Bottom). Thus stabilization of Yhp1-mkb/mdb resulted in extended repression of *MCM7* and *RNR1* transcription.

Given that stabilized versions of Yhp1 and Nrm1 had adverse effects on G1 transcription, we wondered whether they would also retard cell growth. Since there was no obvious growth defect on plates, we performed coculture experiments, which have greater sensitivity. Thus, wild-type and *nrm1-mdb* mutant strains were genetically marked and grown together, revealing that *nrm1-mdb* cells grew markedly more slowly than wild-type cells (Figure 7A). In contrast, rendering Nrm1 nonfunctional via deletion had no significant effect on growth when compared with *NRM1* cells (unpublished data).

We performed a similar analysis of *YHP1*. Deletion of *YHP1* had no significant impact on cell growth in a coculture experiment. In contrast, *yhp1-mkb/mdb* cells were rapidly displaced from the culture by cells expressing *YHP1*, indicating that expression of stabilized Yhp1 had an adverse effect on cell growth (Figure 7B). Thus stabilization of both Nrm1 and Yhp1 inhibited cell proliferation. The reduction in fitness of cells expressing stabilized Nrm1 was 2.1% per generation, and the reduction in fitness of cells expressing stabilized Yhp1 was 1.8% per generation.

DISCUSSION

By systematically analyzing proteins expressed at the same times as known APC substrates, we identified several novel APC substrates, providing insight into additional cell cycle processes regulated by the APC. We focused on two of these proteins, Nrm1 and Yhp1, which are cell cycle–regulated transcriptional repressors. Both Nrm1

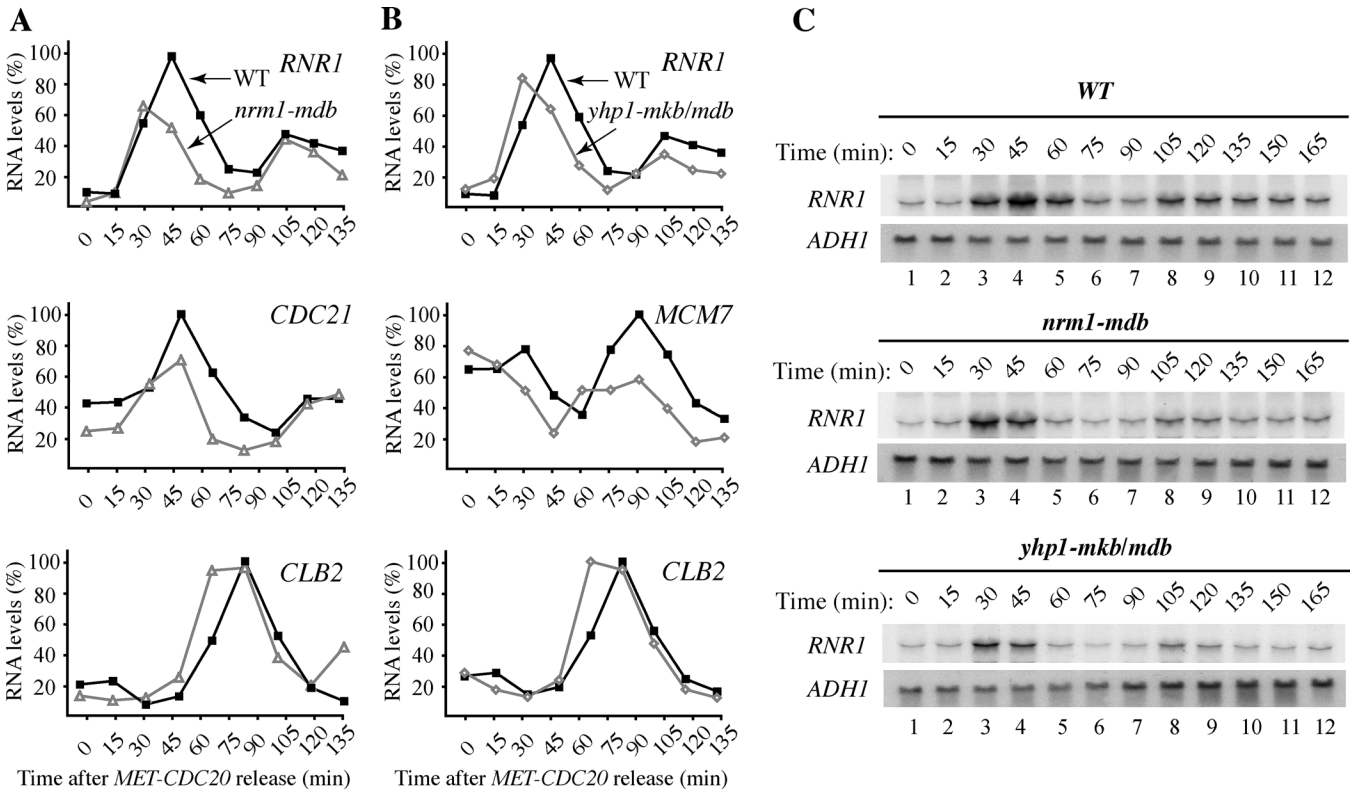

FIGURE 6: Nrm1 and Yhp1 degradation are required for proper G1 transcription. (A, B) Wild-type, *nrm1-mdb*, and *yhp1-mkb/mdb* strains were synchronized in M phase by *CDC20* depletion, as in Figure 4B. Samples were withdrawn every 15 min after release and processed for quantitative reverse transcriptase PCR (qRT PCR) analysis with primers corresponding to *RNR1*, *CDC21*, *MCM7*, and *CLB2*. The relative level of each transcript was normalized to *ACT1* mRNA in the same cells. (C) Northern blot analysis using ^{32}P-labeled probes corresponding to *RNR1* and *ADH1* (for normalization).

and Yhp1 were present at ~10-fold-higher levels during mitosis than in G1, unstable in G1, stabilized by inactivation of the APC, and destabilized following expression of the constitutively active Cdh1-m11 protein. Both also contained identifiable degradation motifs, the mutation of which stabilized the protein.

A major finding of this study was the identification of two unrelated transcriptional repressors as APC substrates. Nrm1- and Yhp1-mediated repression of the MBF and Mcm1 transcription factors, respectively, ensures that G1-specific genes remain silent during other phases of the cycle. Both repressors are cell cycle–regulated, with peak mRNA expression in late G1 (Nrm1) and in S phase (Yhp1). Significantly, Nrm1- and Yhp1-mediated inhibition must be relieved in the next G1 phase to allow gene expression. Previous studies suggested that Nrm1 and Yhp1 were unstable (Pramila *et al.*, 2002; de Bruin *et al.*, 2006); we found that they can both be stabilized, at least partially, in *cdh1*Δ cells and by mutations within degradation motifs. Furthermore, both proteins were efficiently ubiquitinated by purified APC^{Cdh1} in vitro in a D-box-dependent manner. Finally, stabilization of Nrm1 and Yhp1 reduced the cell cycle window during which MBF- and Mcm1-induced genes were expressed, leading to a reduction in cell fitness.

A growing number of transcription factors have been found to be APC substrates. The human transcription factors FoxM1, HOXC10, and AML1/RUNX1 are all targeted by both APC^{Cdc20} and APC^{Cdh1} (Gabellini *et al.*, 2003; Biggs *et al.*, 2006; Park *et al.*, 2008). The APC is also involved in degrading the SnoN and Ume6 transcriptional repressors, which inhibit the transcription of TGF-β–responsive genes in human cells and of meiosis-specific genes in yeast, respectively (Wan *et al.*, 2001; Mallory *et al.*, 2007). Taken together with our findings on Nrm1 and Yhp1, these examples illustrate an emerging theme in which the APC helps coordinate transcription of large sets of genes by promoting the degradation of transcriptional repressors.

Interestingly, Yhp1 appears to be degraded by at least two pathways, including a non-APC mechanism during M phase followed by APC-mediated degradation to eliminate residual Yhp1 as cells enter G1. Cyclin Clb5 is also targeted by a second pathway, leading to only partial stabilization under certain conditions following APC inactivation (Sari *et al.*, 2007). This second pathway may be important for the degradation of Yhp1 in late mitosis, which allows Mcm1-dependent transcription of a set of early cell cycle genes, including *CLN3*. In contrast, MBF activity is restricted to middle G1, so Nrm1 degradation in early G1 by APC^{Cdh1} is sufficient.

We found that Nrm1 appears to be stabilized via phosphorylation, likely carried out by Cdc28. Thus Nrm1 was significantly destabilized upon inactivation of Cdc28 or when Cdk consensus sites within Nrm1 were mutated to alanines. Furthermore, substitutions that mimicked phosphorylated amino acids within Cdk consensus sites increased Nrm1 stability. Presumably, the initial drop of Cdc28 activity in early G1 leads to Nrm1 dephosphorylation, which exposes Nrm1 for Cdh1-mediated degradation. The stabilization of Nrm1 by Cdc28 may subsequently serve to stabilize Nrm1 during the latter part of G1, when APC^{Cdh1} is still active and most APC^{Cdh1} substrates are still unstable. Similar dual regulation has also been described for Mps1 and Cdc5 (Jaspersen *et al.*, 2004; Crasta *et al.*, 2006), and for Pds1/securin, where phosphorylation at five Cdk

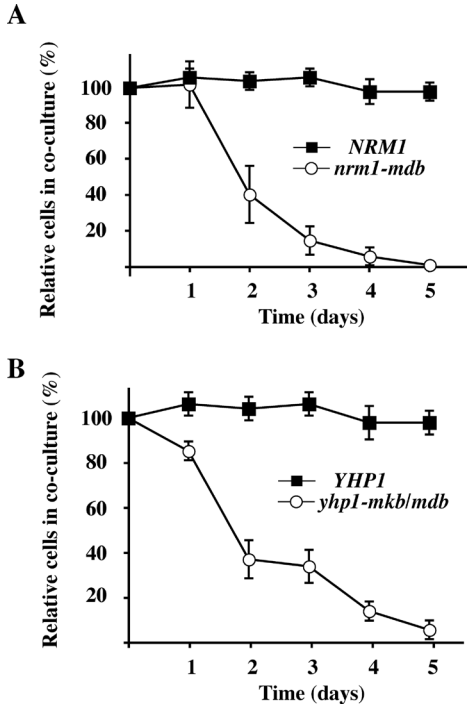

FIGURE 7: Stabilization of Nrm1 and Yhp1 reduces cell fitness. (A) A genetically marked wild-type control strain was grown in coculture with a differentially marked *NRM1* or *nrm1-mdb* test strain for 5 d with dilution of the cocultures once per day. The cultures were tested daily for the presence of *TRP1* and *LEU2* auxotrophs by plating on selective medium. The markers of the wild-type control strain and the experimental *NRM1* and *nrm1-mdb* strains were swapped, the coculture experiment was repeated, and the results were averaged as described in *Materials and Methods*. (B) As in (A), but using *YHP1* and *yhp1-mkb/mdb* test strains.

sites, including two sites in close proximity to KEN- and D-boxes, protects Pds1 from APC^{Cdc20} (Holt *et al.*, 2008). It remains to be determined whether such phosphorylation serves in general to allow APC substrate accumulation while APC^{Cdh1} is still active.

A number of screens have been performed to identify novel APC substrates. Remarkably, most new substrates were identified in just a single screen. Previous attempts included assaying protein ubiquitination in vitro and screening libraries of fluorescently tagged proteins in vivo (Benanti *et al.*, 2009; Merbl and Kirschner, 2009). These approaches favored the identification of high-abundance substrates. Our strategy involved the identification of candidates based on the similarity of their transcriptional profiles with those of known APC substrates, followed by an analysis of individual candidates. Although we identified a good number of new substrates, perhaps an equal number may have been missed for a variety of reasons. First, we examined only those proteins among the ~80% of the genome represented in the TAP-tag library (Ghaemmaghami *et al.*, 2003). Second, very-low-abundance substrates may not have been detected on the immunoblots. Third, it is possible that some APC substrates are not encoded by cell cycle–regulated transcripts. Finally, few screens (including the current one) would have identified meiotic APC substrates. It is also worth noting that our screen appears to have a bias toward the identification of APC^{Cdh1} substrates over APC^{Cdc20} substrates.

The degradation of only two APC substrates in yeast is essential. Cells expressing stabilized forms of either Pds1 (securin) or Clb2 (a mitotic cyclin) arrest permanently. The degradation of all other APC substrates is nonessential, as is Cdh1 itself, though such cells grow slowly. On superficial analysis, stabilization of Nrm1 and Yhp1 do not cause major cell cycle delays. However, as shown in our coculture experiments, stabilization of Nrm1 or Yhp1 reduces cell fitness by 1.8–2.1% per generation. Though corresponding to just a 1.6- to 1.9-min lengthening of the cell cycle, these reductions are enough to quickly eliminate such strains from a population. Collectively, the degradation of a number of such "minor" substrates can have a very great effect on the viability of a strain, particularly in a competitive situation in the wild.

MATERIALS AND METHODS

Yeast strains and plasmids

Yeast strains were derivatives of W303a (*ade2-1 trp1-1 leu2-3112 his3-11,15 ura3-1*); their relevant genotypes are listed in Supplemental Table II. Conditional *cdc23-1* and *cdc15-2* strains were described previously (Burton and Solomon, 2000). The *MET-CDC20* strain was provided by Angelika Amon (MIT, Cambridge, MA; D'Aquino *et al.*, 2005), the *cdh1-m11* strain was provided by Wolfgang Seufert (University of Stuttgart, Stuttgart, Germany; Zachariae *et al.*, 1998), the *cdc28-as* analogue-sensitive strain was provided by David Morgan (University of California, San Francisco, CA; Bishop *et al.*, 2000), and the yeast two-hybrid strain was provided by Stan Fields (University of Washington, Seattle, WA; James *et al.*, 1996). Construction of the *nrm1*Δ (W303a *nrm1::natMX4*) and *yhp1*Δ (W303a *yhp1::natMX4*) strains was accomplished by a PCR-based method (Goldstein and McCusker, 1999). Gene disruptions were verified by PCR using a primer downstream of the deleted gene and a primer internal to *natMX4*.

NRM1-TAP and *YHP1-TAP* were amplified from the TAP library (Ghaemmaghami *et al.*, 2003) and cloned into YCplac22 GALp (Gietz and Sugino, 1988). The resulting plasmids were used as templates to introduce mutations within putative regulatory motifs. For *NRM1*, the following mutations were introduced: ^{7}RLPL → ^{7}ALPA (*nrm1-mdb*); ^{163}TPAR → ^{163}APAR, ^{171}TPSS → ^{171}APSS, ^{207}TPIR → ^{207}APIR, ^{231}TPTS → ^{231}APTS (*nrm1–4TA*); and ^{163}TPAR → ^{163}DPAR, ^{171}TPSS → ^{171}DPSS, ^{207}TPIR → ^{207}DPIR, ^{231}TPTS → ^{231}DPTS (*nrm1–4TD*). *YHP1* was altered within two degradation motifs: ^{329}KEN → ^{329}AAA, ^{340}RKPL → ^{340}AKPA (*yhp1-mkb/mdb*). All mutations were verified by sequencing of the entire coding region. Primer sequences and further details of the plasmids are available upon request.

Cell growth and arrest conditions

Cultures were grown in yeast extract–peptone–dextrose (YPD) and in complete minimal (CM) media, as previously described (Guthrie and Fink, 1991). Cells of *bar1*Δ strains were arrested in G1 phase with 100 ng/ml α-factor or in M phase with 20 μg/ml benomyl for 2 h at 30°C. For cell cycle synchronization, *MET-CDC20*-expressing cells were incubated with 5 mM methionine for 2 h at 30°C; cells were washed by filtration (Corning Filter System, Lowell, MA) and released into prewarmed methionine-free medium. Alternatively, *cdc15-2* cells were arrested in anaphase by incubation at 37°C for 3 h followed by release at 23°C. For analyses of protein stability, cells were grown in yeast extract–peptone–Raffinose to midexponential phase (OD_{600} ~0.4). Galactose was added to 2% for 50 min at 30°C, followed by addition of 500 μg/ml cycloheximide (MP Biomedicals, Solon, OH) and 2% dextrose, as previously described (Ostapenko *et al.*, 2008).

For coculture experiments, wild-type and mutant strains differentially marked with either *TRP1* and *LEU2* were grown together in YPD supplemented with 50 μg/ml of tryptophan and leucine at 23°C

to OD_{600} ~1.0. The cocultures were diluted 1000-fold into fresh medium each day and propagated for 5 d. Aliquots were plated daily onto CM-Trp and CM-Leu plates to determine the percentage of each type of cell in the coculture. For each comparison, the *TRP1* and *LEU2* markers of the two strains were then swapped, the coculture repeated, and the results averaged.

Yeast extracts and immunoblotting

Yeast cell extracts were prepared by shaking yeast suspensions with glass beads, as previously described (Ostapenko *et al.*, 2008). For detection of low-abundance proteins, TAP-tagged proteins were precipitated with IgG-Sepharose (GE Healthcare, Waukesha, WI), separated by SDS–PAGE, and transferred to an Immobilon-P membrane (Millipore, Billerica, MA). The membranes were probed with peroxidase–antiperoxidase (PAP, 1.3 µg/ml; Sigma-Aldrich, St. Louis, MO) and proteins were visualized by chemiluminescence (SuperSignal, Pierce, Thermo Scientific, Lafayette, CO).

Ubiquitination assays

The APC was purified from YJB910 (*MATa pep4-3 his3-Δ1 leu2-3112 CDC16-TAP::CDC16 APC4-HA::APC4*) using a single-step TAP-affinity purification, as previously described (Dial *et al.*, 2007). Briefly, 5 l of YJB910 cells were grown in YPD to OD_{600} = 1.0. Cells were lysed using a French Press (Thermo Scientific) in 25 mM HEPES, pH 7.5, 150 mM NaCl, 10% glycerol, 0.1% IgepalCAG30, 0.1 mM dithiothreitol (DTT), 0.5 mM phenylmethylsulfonyl fluoride (PMSF), and 10 µg each of leupeptin, chymostatin, and pepstatin (Chemicon, Millipore). The cell extract was clarified by ultracentrifugation at 40,000 rpm in a Ti60 rotor (Beckman, Brea, CA) for 30 min at 4°C, supplemented with 2 mM $CaCl_2$, and the TAP-associated proteins were purified using 0.5 ml bed volume of Calmodulin-Sepharose resin (GE Healthcare). Bound proteins were eluted with 10 mM Tris-HCl, pH 8.0, 150 mM NaCl, 10% glycerol, 1 mM $MgCl_2$, 2 mM EGTA, 0.1% IgepalCAG30, 3 mM DTT, and 10 µg each of leupeptin, chymostatin, and pepstatin (Chemicon, Millipore). The purified APC was aliquoted and stored at a concentration of 0.1 mg/ml at –80°C. Recombinant 6XHis-Cdh1 was purified from baculovirus-infected cells (Burton *et al.*, 2005); 6XHis-Uba1 and 6XHis-Ubc4 proteins were purified from yeast and bacterial extracts, respectively, on Talon resin, as previously described (Ostapenko *et al.*, 2008).

^{35}S-Nrm1 and ^{35}S-Yhp1 were prepared by translation in vitro using the TNT T7 quick-coupled transcription/translation system (Promega, Madison, WI) according to the manufacturer's instructions in the presence of 3 µl (30 µCi) [^{35}S]methionine (GE Healthcare). Ubiquitination assays were conducted in the presence or absence of 2.5 µg 6XHis-Cdh1/100 ng purified APC and contained 3.0 µg 6XHis-Uba1, 5.0 µg 6XHis-Ubc4, 150 µM bovine ubiquitin (Sigma-Aldrich), 1 mM ATP (Sigma-Aldrich), 1x ubiquitination buffer (40 nM Tris-HCl, pH 7.6, 10 mM $MgCl_2$, and 0.6 mM DTT) and 2 µl ^{35}S-labeled substrate in a 15-µl volume and were carried out for 10 min at 23°C essentially as described (Carroll *et al.*, 2005). The reaction products were separated by SDS–PAGE and visualized by autoradiography.

RNA analyses

Total RNA was isolated from yeast cells using an acid lysis protocol as described (Ostapenko and Solomon, 2003). The DyNAmo SYBR Green qRT-PCR kit (NEB, Ipswich, MA) was used for quantitative RT-PCR. Reactions were run on an API Prism system (Applied Biosystems, Bedford, MA) under standard RT-PCR conditions using the following primer pairs: MSO2991/2992 (*ACT1*), MSO2993/2994 (*CDC21*), MSO2995/2996 (*CLB2*), MSO3003/3004 (*RNR1*), MSO3028/3029 (*MCM7*). Primer sequences are available upon request. All data were normalized to *ACT1* levels in the same cells. For Northern hybridization analysis, 20 µg RNA was electrophoresed in 1% formaldehyde-agarose gels and transferred to Hybond-N membranes (GE Healthcare). PCR fragments corresponding to *RNR1* and *ADH1* were labeled with α-^{32}P-dCTP (NEN, PerkinElmer, Waltham, MA) using the Prime It II kit (Stratagene, Agilent, Santa Clara, CA) and hybridized to the membranes for 10 h at 42°C according to the manufacturer's protocol. Bands were visualized by autoradiography and phosphorimaging (PhosphorImager, Molecular Dynamics, Sunnyvale, CA).

ACKNOWLEDGMENTS

We thank Janet Burton for the Cdh1 two-hybrid vector and Angelika Amon, Stan Fields, David Morgan, and Wolfgang Seufert for strains. We thank Janet Burton, Mark Hochstrasser, and Ruiwen Wang for critical reading of the manuscript and helpful discussions. This work was supported by grants GM076200 and GM088272 from the National Institutes of Health and by research grant 1-FY05-114 from the March of Dimes Foundation awarded to M.J.S.

REFERENCES

Belle A, Tanay A, Bitincka L, Shamir R, O'Shea EK (2006). Quantification of protein half-lives in the budding yeast proteome. Proc Natl Acad Sci USA 103, 13004–13009.

Benanti JA, Matyskiela ME, Morgan DO, Toczyski DP (2009). Functionally distinct isoforms of Cik1 are differentially regulated by APC/C-mediated proteolysis. Mol Cell 33, 581–590.

Biggs JR, Peterson LF, Zhang Y, Kraft AS, Zhang DE (2006). AML1/RUNX1 phosphorylation by cyclin-dependent kinases regulates the degradation of AML1/RUNX1 by the anaphase-promoting complex. Mol Cell Biol 26, 7420–7429.

Bishop AC *et al.* (2000). A chemical switch for inhibitor-sensitive alleles of any protein kinase. Nature 407, 395–401.

Burton JL, Solomon MJ (2000). Hsl1p, a Swe1p inhibitor, is degraded via the anaphase-promoting complex. Mol Cell Biol 20, 4614–4625.

Burton JL, Solomon MJ (2001). D box and KEN box motifs in budding yeast Hsl1p are required for APC-mediated degradation and direct binding to Cdc20p and Cdh1p. Genes Dev 15, 2381–2395.

Burton JL, Solomon MJ (2007). Mad3p, a pseudosubstrate inhibitor of APC^{Cdc20} in the spindle assembly checkpoint. Genes Dev 21, 655–667.

Burton JL, Tsakraklides V, Solomon MJ (2005). Assembly of an APC-Cdh1-substrate complex is stimulated by engagement of a destruction box. Mol Cell 18, 533–542.

Carroll CW, Enquist-Newman M, Morgan DO (2005). The APC subunit Doc1 promotes recognition of the substrate destruction box. Curr Biol 15, 11–18.

Chua G, Morris QD, Sopko R, Robinson MD, Ryan O, Chan ET, Frey BJ, Andrews BJ, Boone C, Hughes TR (2006). Identifying transcription factor functions and targets by phenotypic activation. Proc Natl Acad Sci USA 103, 12045–12050.

Crasta K, Huang P, Morgan G, Winey M, Surana U (2006). Cdk1 regulates centrosome separation by restraining proteolysis of microtubule-associated proteins. EMBO J 25, 2551–2563.

D'Aquino KE, Monje-Casas F, Paulson J, Reiser V, Charles GM, Lai L, Shokat KM, Amon A (2005). The protein kinase Kin4 inhibits exit from mitosis in response to spindle position defects. Mol Cell 19, 223–234.

de Bruin RA, Kalashnikova TI, Chahwan C, McDonald WH, Wohlschlegel J, Yates J 3rd, Russell P, Wittenberg C (2006). Constraining G1-specific transcription to late G1 phase: the MBF-associated corepressor Nrm1 acts via negative feedback. Mol Cell 23, 483–496.

Di Fiore B, Pines J (2007). Emi1 is needed to couple DNA replication with mitosis but does not regulate activation of the mitotic APC/C. J Cell Biol 177, 425–437.

Dial JM, Petrotchenko EV, Borchers CH (2007). Inhibition of APC^{Cdh1} activity by Cdh1/Acm1/Bmh1 ternary complex formation. J Biol Chem 282, 5237–5248.

Enquist-Newman M, Sullivan M, Morgan DO (2008). Modulation of the mitotic regulatory network by APC-dependent destruction of the Cdh1 inhibitor Acm1. Mol Cell 30, 437–446.

Fang G, Yu H, Kirschner MW (1998). The checkpoint protein MAD2 and the mitotic regulator CDC20 form a ternary complex with the anaphase-promoting complex to control anaphase initiation. Genes Dev 12, 1871–1883.
Gabellini D, Colaluca IN, Vodermaier HC, Biamonti G, Giacca M, Falaschi A, Riva S, Peverali FA (2003). Early mitotic degradation of the homeoprotein HOXC10 is potentially linked to cell cycle progression. EMBO J 22, 3715–3724.
Ghaemmaghami S, Huh WK, Bower K, Howson RW, Belle A, Dephoure N, O'Shea EK, Weissman JS (2003). Global analysis of protein expression in yeast. Nature 425, 737–741.
Gietz RD, Sugino A (1988). New yeast-*Escherichia coli* shuttle vectors constructed with in vitro mutagenized yeast genes lacking six-base pair restriction sites. Gene 74, 527–534.
Glotzer M, Murray AW, Kirschner MW (1991). Cyclin is degraded by the ubiquitin pathway. Nature 349, 132–138.
Goldstein AL, McCusker JH (1999). Three new dominant drug resistance cassettes for gene disruption in *Saccharomyces cerevisiae*. Yeast 15, 1541–1553.
Guthrie C, Fink GR (1991). Guide to Yeast Genetics and Molecular Biology, San Diego, CA: Academic Press.
Hildebrandt ER, Hoyt MA (2001). Cell cycle-dependent degradation of the *Saccharomyces cerevisiae* spindle motor Cin8p requires APC(Cdh1) and a bipartite destruction sequence. Mol Biol Cell 12, 3402–3416.
Holt LJ, Krutchinsky AN, Morgan DO (2008). Positive feedback sharpens the anaphase switch. Nature 454, 353–357.
Hwang LH, Lau LF, Smith DL, Mistrot CA, Hardwick KG, Hwang ES, Amon A, Murray AW (1998). Budding yeast Cdc20: a target of the spindle checkpoint. Science 279, 1041–1044.
James P, Halladay J, Craig EA (1996). Genomic libraries and a host strain designed for highly efficient two-hybrid selection in yeast. Genetics 144, 1425–1436.
Jaspersen SL, Charles JF, Morgan DO (1999). Inhibitory phosphorylation of the APC regulator Hct1 is controlled by the kinase Cdc28 and the phosphatase Cdc14. Curr Biol 9, 227–236.
Jaspersen SL, Huneycutt BJ, Giddings TH Jr, Resing KA, Ahn NG, Winey M (2004). Cdc28/Cdk1 regulates spindle pole body duplication through phosphorylation of Spc42 and Mps1. Dev Cell 7, 263–274.
Juang YL, Huang J, Peters JM, McLaughlin ME, Tai CY, Pellman D (1997). APC-mediated proteolysis of Ase1 and the morphogenesis of the mitotic spindle. Science 275, 1311–1314.
Kerscher O, Felberbaum R, Hochstrasser M (2006). Modification of proteins by ubiquitin and ubiquitin-like proteins. Annu Rev Cell Dev Biol 22, 159–180.
Kimata Y, Baxter JE, Fry AM, Yamano H (2008a). A role for the Fizzy/Cdc20 family of proteins in activation of the APC/C distinct from substrate recruitment. Mol Cell 32, 576–583.
Kimata Y, Trickey M, Izawa D, Gannon J, Yamamoto M, Yamano H (2008b). A mutual inhibition between APC/C and its substrate Mes1 required for meiotic progression in fission yeast. Dev Cell 14, 446–454.
Ko N, Nishihama R, Tully GH, Ostapenko D, Solomon MJ, Morgan DO, Pringle JR (2007). Identification of yeast IQGAP (Iqg1p) as an anaphase-promoting-complex substrate and its role in actomyosin-ring-independent cytokinesis. Mol Biol Cell 18, 5139–5153.
Mallory MJ, Cooper KF, Strich R (2007). Meiosis-specific destruction of the Ume6p repressor by the Cdc20-directed APC/C. Mol Cell 27, 951–961.
Merbl Y, Kirschner MW (2009). Large-scale detection of ubiquitination substrates using cell extracts and protein microarrays. Proc Natl Acad Sci USA 106, 2543–2548.
Ostapenko D, Burton JL, Wang R, Solomon MJ (2008). Pseudosubstrate inhibition of the anaphase-promoting complex by Acm1: regulation by proteolysis and Cdc28 phosphorylation. Mol Cell Biol 28, 4653–4664.
Ostapenko D, Solomon MJ (2003). Budding yeast CTDK-I is required for DNA damage-induced transcription. Eukaryot Cell 2, 274–283.
Park HJ, Costa RH, Lau LF, Tyner AL, Raychaudhuri P (2008). Anaphase-promoting complex/cyclosome-CDH1-mediated proteolysis of the forkhead box M1 transcription factor is critical for regulated entry into S phase. Mol Cell Biol 28, 5162–5171.
Peters JM (2006). The anaphase promoting complex/cyclosome: a machine designed to destroy. Nat Rev Mol Cell Biol 7, 644–656.
Petroski MD, Deshaies RJ (2005). Function and regulation of cullin-RING ubiquitin ligases. Nat Rev Mol Cell Biol 6, 9–20.
Pfleger CM, Kirschner MW (2000). The KEN box: an APC recognition signal distinct from the D box targeted by Cdh1. Genes Dev 14, 655–665.
Pramila T, Miles S, GuhaThakurta D, Jemiolo D, Breeden LL (2002). Conserved homeodomain proteins interact with MADS box protein Mcm1 to restrict ECB-dependent transcription to the M/G1 phase of the cell cycle. Genes Dev 16, 3034–3045.
Pramila T, Wu W, Miles S, Noble WS, Breeden LL (2006). The Forkhead transcription factor Hcm1 regulates chromosome segregation genes and fills the S-phase gap in the transcriptional circuitry of the cell cycle. Genes Dev 20, 2266–2278.
Reimann JD, Gardner BE, Margottin-Goguet F, Jackson PK (2001). Emi1 regulates the anaphase-promoting complex by a different mechanism than Mad2 proteins. Genes Dev 15, 3278–3285.
Sari F, Braus GH, Irniger S (2007). A process independent of the anaphase-promoting complex contributes to instability of the yeast S phase cyclin Clb5. J Biol Chem 282, 26614–26622.
Shirayama M, Zachariae W, Ciosk R, Nasmyth K (1998). The Polo-like kinase Cdc5p and the WD-repeat protein Cdc20p/fizzy are regulators and substrates of the anaphase promoting complex in *Saccharomyces cerevisiae*. EMBO J 17, 1336–1349.
Spellman P, Sherlock G, Zhang M, Iyer V, Anders K, Eisen M, Brown P, Botstein D, Futcher B (1998). Comprehensive identification of cell cycle-regulated genes of the yeast *Saccharomyces cerevisiae* by microarray hybridization. Mol Biol Cell 9, 3273–3297.
Thornton BR, Ng TM, Matyskiela ME, Carroll CW, Morgan DO, Toczyski DP (2006). An architectural map of the anaphase-promoting complex. Genes Dev 20, 449–460.
Thornton BR, Toczyski DP (2003). Securin and B-cyclin/CDK are the only essential targets of the APC. Nat Cell Biol 5, 1090–1094.
Ubersax JA, Woodbury EL, Quang PN, Paraz M, Blethrow JD, Shah K, Shokat KM, Morgan DO (2003). Targets of the cyclin-dependent kinase Cdk1. Nature 425, 859–864.
Wan Y, Liu X, Kirschner MW (2001). The anaphase-promoting complex mediates TGF-beta signaling by targeting SnoN for destruction. Mol Cell 8, 1027–1039.
Woodbury EL, Morgan DO (2007). Cdk and APC activities limit the spindle-stabilizing function of Fin1 to anaphase. Nat Cell Biol 9, 106–112.
Yu H (2002). Regulation of APC-Cdc20 by the spindle checkpoint. Curr Opin Cell Biol 14, 706–714.
Zachariae W, Schwab M, Nasmyth K, Seufert W (1998). Control of cyclin ubiquitination by CDK-regulated binding of Hct1 to the anaphase promoting complex. Science 282, 1721–1724.